Published in : Journal of Constructional Steel Research 235 (2025) 109916
DOI:10.1016/j.jcsr.2025.109916
Status : Postprint (Author's version)

Seismic design and testing of EC8-1-2-compliant unstiffened end-plate beam-to-column joints

Roberto Tartaglia [a], Mario D'Aniello [b], Jean-François Demonceau [c], Raffaele Landolfo [d,*]

[a] *Department of Engineering, University of Sannio, Piazza Roma 21, 82100 Benevento, Italy*

[b] *Department of Structures for Engineering and Architecture, University of Naples "Federico II", Via Forno Vecchio 36, 80134 Naples, Italy*

[c] *UEE Research Unit, University of Liege, Belgium*

[d] *Department of Structures for Engineering and Architecture, University of Naples "Federico II", Via Forno Vecchio 36, 80134 Naples, Italy*

Keywords:
Steel bolted joints
Partial strength joints
Extended unstiffened end-plate connection
Seismic design
Moment-rotation response
FEM analysis

ABSTRACT

Cyclic tests and finite element simulations were carried out to investigate the performance of partial strength unstiffened end-plate joints that have been designed either for moment frames in low seismic areas or to provide redundancy, ductility, and extra dissipation capacity of dual frames (i.e., braced frames as primary seismic resisting system in combination with moment frames as secondary system) in the framework of the second generation of Eurocode 8. The tested joints have been designed to promote yielding in the end-plate connection and the column web panel in shear, while preventing the failure of the bolts and welds in the range of the required plastic rotation for highly ductile structures. Three beam-to-column assemblies have been considered to account for the influence of the size of members. Moreover, the tested specimens were designed to vary the relative resistances of the column web panel and connection as follows: (i) balanced column web panel and equal strength connection, (ii) balanced column web panel and partial strength connection, (iii) weak column web panel and equal strength connection, (iv) weak column web panel and partial strength connection. The adopted design criteria of the tested joints are described, and the main technological details are also reported. The tested joints were also numerically investigated using finite element simulations. The accuracy of advanced numerical models was verified against the performed experimental tests, and the validated models were used to investigate the local response of the joints, thus highlighting the influence of both geometrical and mechanical parameters.

Published in : Journal of Constructional Steel Research 235 (2025) 109916
DOI:10.1016/j.jcsr.2025.109916
Status : Postprint (Author's version)

List of symbols

C_{pr}	Strain hardening factor provided by AISC358–16	y_c	Specified minimum yield stress of the column
E	Young modulus of steel	f_{yp}	Specified minimum yield stress of the end-plate
L_h	Distance between plastic hinges	g	Horizontal distance (gage) between fastener lines
$M_{b,pl,k}$	Beam plastic bending capacity	g_{0e}	Horizontal distance (gage) between outer bolts of the two bolt rows outside the beam flange in the 8EM joint
$M_{con,Rd}$	Bending capacity of the connection	g_{0i}	Horizontal distance (gage) between outer bolts of the two bolt rows inside the beam flange in the 8EM joint
$M_{con,Rd}$	Bending capacity of the connection	h_0	Distance between the centre of the outer bolt row and the compression centre
$M_{cwp,\ Rd}$	Bending capacity of the panel zone	h_{EP}	End-plate height
M_{Ed}	Design moment at the column face also evaluated considering the strain hardening factor and the randomness material factor	h_i	Distance between the centre of the bolt row i and the compression centre
$M_{Ed,\ CF}$	Design moment at the column face evaluated without the strain hardening factor and the randomness material factor	h_{st}	Height of end-plate stiffeners
Mj,Rd	Design moment resistance of the joint	k and k'	Out-of-square of the flange tips of the hot-rolled profiles;
M_{pr}	Probable maximum moment at the plastic hinge	m	The distance from the centre of a fastener to either a fillet weld or the radius of a rolled section fillet (measured at a depth within the fillet equal to 20 % of its size).
M_{Rd}	Bending capacity of the joint, calculated as min(Mcon,Rd; MRd, web)	p_1	Spacing between the first and the second active bolt row
M_u	Ultimate bending capacity of the joint	p_2	Spacing between the second and the third active bolt row
M_y	Yield capacity of the joint	p_b	Vertical distance between the inner and outer row of bolts in the eight-bolt stiffened extended end-plate moment connection
S_j	Joint stiffness	p_{be}	Vertical distance between outer row of bolts in 8EM connection
$V_{Ed,G}$	Shear force associated with the non-seismic actions	p_{bi}	Vertical distance between inner row of bolts in 8EM connection
$V_{Ed,M}$	Shear force associated with the formation of plastic hinges	p_f	vertical distance from beam flange edge to nearest bolt row
$V_{gravity}$	Beam shear force due to gravity loads	s	Distance from the centreline of either the most inside or most outside tension bolt row to the edge of a yield line pattern
V_u	Shear force acting in the section where the plastic hinge forms	$s_{h,c}$	Distance between the plastic hinge and the column face
$V_{wp,Ed}$	Shear force in the web panel	t_c	Column flange thickness
$V_{wp,Rd}$	Shear resistance of the web panel	$t_{c,req}$	Required column flange thickness
Y_c	Column yield line mechanism parameter	$t_{c,w}$	Thickness of the column web
Y_{cs}	Stiffened column yield line mechanism parameter	t_{cp}	Thickness of the continuity plate
Y_{cu}	Unstiffened column yield line mechanism parameter	t_{EP}	End-plate thickness
Y_p	End-plate yield line mechanism parameter	$t_{p,req}$	Required end-plate thickness
b_{cf}	Column flange width	t_{st}	Thickness of end-plate stiffeners
b_{EP}	End-plate width	t_{wb}	Thickness of the beam web
b_f	Beam flange width	w	Horizontal distance between bolts
d	Bolt diameter	γ_{ov}	Joint over-strength factor
d_b	Depth of the beam	γ_{rm}	Randomness material factor (assumed equal to 1.25)
$d_{b,req}$	Required bolt diameter	γ_{sh}	Strain hardening coefficient
$d_{c,w}$	Depth of the column web	ε^p_{ij}	Tensor of plastic strains
d_e	Vertical distance between the outer bolt row and the edge of the end-plate or the column	ε_y	Tensor of uniaxial yield strains
e	Distance from the centre of a fastener to the nearest edge	$\theta_{0.8Mp}$	Rotation at a capacity equal to 80 % of the plastic flexural resistance of the beam
f_{nt}	Nominal tensile strength of the bolt	θ_p	Plastic rotation
f_u	Specified minimum tensile stress of the yielding element	θ_u	Ultimate rotation
f_{ub}	Specified ultimate tensile stress of the bolt	θ_y	Yield rotation
f_y	Specified minimum yield stress of the yielding element	σ_e	The Von Mises stress
$f_{y,st}$	Specified minimum yield stress of end-plate stiffeners	σ_m	The hydrostatic stress
$f_{y,w}$	Specified tensile yield strength of the material of the column web panel	ϕ_d	Resistance factor for ductile limit states
f_{yb}	Specified minimum yield stress of the beam	ϕ_n	Resistance factor for nondductile limit states

Published in : Journal of Constructional Steel Research 235 (2025) 109916
DOI:10.1016/j.jcsr.2025.109916
Status : Postprint (Author's version)

1. Introduction

Unstiffened end-plate (UEP) joints are regularly used as primary moment-resisting joints in numerous countries, particularly in European steel moment-resisting structures. These joints can behave in a ductile manner provided that their collapse mechanisms are not characterised by either the failure of the welds (if fillet welds are used to connect the beam flange in tension and the end-plate) or the bolts [1]. However, excessive flexibility and envisaged concentration of ductility demand suggest using UEP for moment frames in low-seismic areas. Conversely, in dual frames (i.e., braced frames as primary seismic resisting system in combination with moment frames) the moment resisting sub-system can provide redundancy to avoid soft storey mechanisms (which typically characterise the seismic response of pure braced systems), especially if the moment resisting bays are not included in the braced bays.

Therefore, in dual systems, the moment resisting bays are intended to be activated as a secondary mechanism, and limited ductility demand is expected in the moment connections at the significant damage (i.e., life safety) limit state. Under this condition, ductile damage of the beam-to- column connection and panel zone can be intentionally promoted to have cheaper constructional details (i.e., in comparison to a full strength connection, a weak connection would require thinner end-plate, smaller and fewer number of bolts, no stiffeners, etc.).

End-plate connections are commonly analysed and designed using the analogy with an equivalent T-stub [2], and many studies have been conducted to characterise its ductility under static, cyclic, and impact loading conditions [3–11].

In Europe, these joints are commonly designed and verified for non- seismic loads in accordance with EN1993–1-8:2005 [12] (also referred to as EC3–1-8 that is the European code for the design of steel joints), which establishes criteria for classifying joints based on their stiffness and strength, and provides rules to estimate their resistance and stiffness for analytical modelling. Some limited guidance is given to ensure the ductility (i.e., rotation capacity) of the joints, as EN1993–1-8 [12], by enforcing the minimum resistances in the ductile components of the joints as follows:

(1) in column web panel (i.e., if the design moment resistance of the joint $M_{j,Rd}$ is governed by the.

design resistance of the column web panel in shear) provided that $d_{c,w}/t_{c,w} \leq 69\varepsilon$ where $d_{c,w}$ is the web depth of the column, $t_{c,w}$ is its thickness, $\varepsilon = \sqrt{235/f_{y,w}}$, and $f_{y,w}$ is the tensile yield strength of the
material of the column web panel;

(2) the beam flange in tension or the column web in tension;

(3) in column flange or end-plate in bending provided that the thickness *t* of either the column flange or the beam end-plate satisfies:

$$t \leq 0,36 \bullet d \bullet \sqrt{\frac{f_{u,b}}{f_{y,p}}} \qquad (1)$$

where *d* is the nominal diameter of the bolt, $f_{u,b}$ is the ultimate tensile strength of the bolt, and $f_{y,p}$ is the tensile yield strength of the material of either the end-plate or the column flange.

As an alternative to requirements (1), (2) and (3), the rotation capacity of a joint has not to be checked for plastic analysis under static loading conditions provided that the $M_{j,Rd}$ is at least 1.2 times the design plastic moment resistance $M_{pl,Rd}$ of the cross-section of the connected beam. This requirement is intended to ensure a full-strength character to the joint, in which case most of the plastic deformations are expected in the beam.

Similar conditions are still given in the latest draft of prEN1993–1-8 (i.e., the draft of the second generation of EC3–1-8, which has just been published at the time of this publication) [13]. Indeed, conditions (1) to (3) for partial strength joints are complemented with the possibility of verifying the ductility through testing in accordance with EN 1990 [14], or (ii) by appropriate calculation models, provided that they are based on the results of tests in accordance with EN 1990 [14]. The case of fullstrength joints has been revised replacing the overstrength factor 1.2 of the connection with the γ_{rm} material overstrength factor, determined as the ratio between the mean and nominal values of yield strength of structural steel at the plastic hinge location.

As it can be observed, although the second generation of EN1993-1-8 [13] offers more guidance on joint ductility for plastic analysis, it assumes elastic-perfectly plastic behaviour, neglecting the effects of strain hardening in yielding components and the variability of their material strength is considered solely for the case of full strength joints at global level, not at the component level. These assumptions can be critical for seismic-resistant structures. To address this, in the latest draft of the second generation of Eurocode 8 [15] (which is the European code for the seismic design of buildings, also referred to as pr EN1998-1-2), additional requirements are provided to enforce ductile and dissipative behaviour under cyclic loading for UEP joints. In particular, the prEN1998-1-2 (also referred to as EC8-1-2 hereinafter) complements the EC3–1-8 classification of joints, specifying that the resistance of joints distinguishes the contribution from the column web panel, the connection and the beam to the whole joint resistance. Although this approach roughly contradicts the consistency of the component method (CM) philosophy given by EN1993–1-8, the EC8–1-2 approximated method allows easier control of the hierarchy of resistances between the joint macro-components, thus controlling the yielding pattern of the joint as demonstrated in previous studies [16–20]. In this regard, Landolfo

Published in : Journal of Constructional Steel Research 235 (2025) 109916
DOI:10.1016/j.jcsr.2025.109916
Status : Postprint (Author's version)

[16] summarised the main findings of Equaljoints and Equaljoints-Plus projects where this approach was initially conceived. Tartaglia et al. [17,18] compared the response of partial and full strength extended stiffened end-plate joints designed in accordance with the philosophy in [16] and those designed according to AISC358 [19]. Tartaglia et al. [20] numerically investigated the local response of end-plate joints, confirming the development of the expected yield pattern into the joints designed according to the philosophy given in [16]. The control of the
yielding sequence is needed to prevent brittle failure modes, but does not necessarily guarantee an appropriate ductility of joints with yielding connection and/or column panel zone, as confirmed by the observations of test results reported in many experimental databases [21–26], which proved similar findings. In the case of seismic conditions, the ductility of connections plays a crucial role in ensuring the seismic performance of steel structures because they can undergo large rotations but shall not experience failure to guarantee the overall stability and energy dissipation of the system.

In the case of joints with dissipative connections, EC8–1-2 recommends that the plastic rotation $\vartheta^{p}{}_{u}{}^{j}$ (i.e., without the elastic contribution of the beam and column) should not be smaller than 0.02 rad in DC2 (i. e., for structures with intermediate ductility) and 0.03 rad in DC3 (i.e., for structures with high ductility). Such rotation capacity requirements can be experimentally verified, which may be impractical or costly. On the other hand, EC8–1-2 provides the normative Annex "E" where seismically prequalified joints guarantee compliance with those requirements. The design rules in EC8–1-2 are mainly derived from the findings of two European-funded research projects [16]: EQUALJOINTS and EQUALJOINTS-Plus (EJ). This article summarises the experimental tests and finite element simulations of UEP joints from the EJ projects, and represents the background of the rules provided by Annex E of EC8–1-2. This manuscript is organised into three sections: (i) the design criteria and technological details of the tested joints; (ii) the experimental program and results; and (iii) a comparison between finite element simulations and experimental outcomes.

Fig. 1. *Geometrical features of the studied UEP joints.*

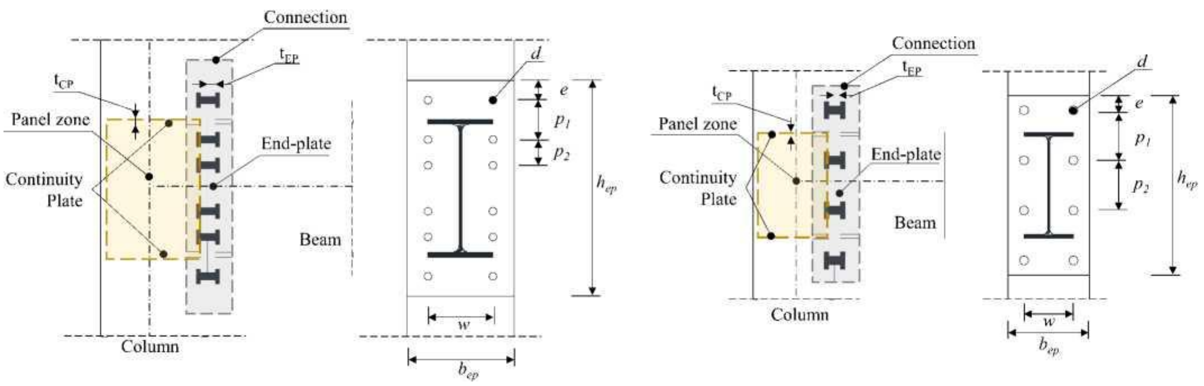

2. Design criteria and technological details

The considered configurations of UEP joints are shown in Fig. 1, namely four bolt rows for joints with shallow beams and six-bolt rows for joints with deep beams. In the six-bolt rows configuration, the inner rows are not aligned to the centroidal axis of the beam in order to (i) contribute to the flexural resistance of the connection, (ii) restrain the opening of the end-plate, (iii) increase the stiffness and limit the plastic demand in both the end-plate and column flange. In the case of connections with shallow beams, any supplementary inner row of bolts could be located only close to the centroidal axis of the beam, which would be ineffective in contributing to the flexural response of the connection.

The investigated UEP joints are designed in accordance with the philosophy of prEN1998-1-2:2022 [15]. Differently from both the first and second generation of EN 1993–1-8 [12,13], in prEN1998-1-2:2022, the required resistance of the connections is evaluated depending on the type and the localisation of the plastic mechanism in the three macrocomponents constituting the beam-to-column joints, namely the beam, the connection and the column web panel [16]. Therefore, accounting for the random material variability and strain hardening of the dissipative zone (i.e., either the beam or the connection), the connections can be categorised on the basis of their resistance as follows:

$M_{con,Rd} \geq \gamma_{rm} \cdot \gamma_{sh} \cdot M_{b,pl,k} + s_{h,c} \cdot V_{EdM}) + s_{h,c} \bullet V_{EdG}$ for full strength connections (2)

$(M_{b,pl,k} + s_{h,c}\, V_{Ed,M}) + s_{h,c}\, V_{Ed,G} \leq M_{con,Rd} < \gamma_{rm} \bullet \gamma_{sh} \bullet (M_{b,pl,k} + s_{h,c}\, V_{Ed,M}) + s_{h,c}\, V_{Ed,G}$ for equal strength connections (3)

Published in : Journal of Constructional Steel Research 235 (2025) 109916
DOI:10.1016/j.jcsr.2025.109916
Status : Postprint (Author's version)

$1/\gamma_{rm}\,[(M_{b,pl,k} + s_{h,c}\,V_{Ed,M}) + s_{h,c}\,V_{Ed,G}\,] \leq M_{con,Rd} < [(M_{b,pl,k} + s_{h,c}\,V_{Ed,M}) + s_{h,c}\,V_{Ed,G}\,]$ for partial strength connections (4)

where:

M_{conRd} is the design resistance of the connection;

$M_{b,pl,k}$ is the nominal plastic moment of the connected beam, i.e. evaluated considering the nominal value of the yield stress f_y of steel;

$V_{Ed,M}$ is the shear force associated to the formation of plastic hinges with nominal plastic resistance at both beam ends (i.e., $V_{Ed,M} = 2\, M_{b,pl,k}/L_h$, L_h being the distance between the plastic hinges at both beam ends);

$V_{Ed,G}$ is the design value of the shear force associated with the non- seismic actions;

$s_{h,c}$ is the distance between the centre of the expected plastic hinge and the connection, which can be simply assumed equal to zero in the case of UEP joints;

γ_{rm} is the randomness material factor (which depends on the steel grade, in accordance with [4]);

γ_{sh} is the strain hardening factor of the plastic hinge (which is assumed equal to 1.2 for flexural yielding as in [15]).

Regarding the column web panel (CWP), prEN1998-1-2:2022 [15] considers three categories depending on the contribution of the column panel zone to the plastic mechanism, namely as follows:

i) strong web panel, where no plastic contribution is required from the column web panel. Accordingly, the plastic contribution is coming from either the connection and/or the beam. In this case, the shear resistance $V_{wp,Rd}$ of the web panel should be taken equal to the resistance of the column web without any additional contribution of continuity plates (if present);

ii) balanced web panel, where plastic contributions are balanced between the column web panel and the connection and/or the beam. In this case, the plastic resistance of the column web zone is also evaluated accounting for the additional resistance of continuity plates (if present) and the shear force $V_{wp,Ed}$ in the web panel is computed considering the minimum moment resistance between the beam and connection;

iii) weak web panel, where all the plastic contribution is coming from the column web panel: it should be designed using the shear force $V_{wp,Ed}$, which is taken as equal to the design moments in the seismic situation divided by the web panel depth.

According to prEN1998-1-2:2022 [15], for full strength connections in the primary structure of moment resisting and dual frames, a strong column web panel should be used. For equal strength connections in the primary structure of moment resisting and dual frames, any type of column web panel may be used. For partial strength connections in the primary structure of moment resisting and dual frames, a balanced or weak column web panel should be used.

In this study, the response of partial strength UEP joints is investigated by varying the resistances of the connection and CWP in order to enforce the demand in the column web panel and investigate its influence on the performance of the welds between the end-plate and beam. Therefore, some specimens were designed with (i) balanced CWP and equal strength connection, (ii) balanced CWP and partial strength connection, (iii) weak CWP and equal strength connection, (iv) weak CWP and partial strength connection.

The theoretical moment resistances of the connections (M_{con}) and CWP (M_{cwp}) are separately estimated according to the simplified assumptions given in [15,16]. In this regard, the design resistance of the connection is mostly calculated in accordance with EN 1993–1-8 with the following complementary assumptions:

(a) the beam web and flange in compression or in tension components are ignored in the calculation of the resistance;

(b) the active bolt rows in tension are those above the central axis of the beam under a hogging moment and below the axis of the beam under a sagging moment, thus the internal equilibrium with the compressive forces and the shear resistance of the CWP is not directly controlled;

The moment Mcwp associated with the shear resistance of the CWP is computed as the product of $V_{wp,Rd}$ (i.e., the shear resistance of CWP including the additional contribution of the continuity plates) and the distance between the centroid of the rigidities of the bolt row in tension and the centre of compression (which is located in the centre of the beam flange in compression). Of course, the resulting resistance of each joint is the smallest between M_{con} and M_{CWP}.

Another considered design condition is the hierarchy between the end-plate and the bolt in tension as recommended by prEN1998-1- 2:2022, which modifies Eq. (1) in order to account for the hardening of the end-plate in bending as follows:

$$t_{EP} \leq 0.30 \bullet d \bullet \sqrt{\frac{f_{u,b}}{f_{y,p}}} \qquad (5)$$

Where the geometrical parameters *tEP* and *d* are defined in Fig. 1, *fu,b* is the ultimate strength of the bolt material and *fy,p*

Published in : Journal of Constructional Steel Research 235 (2025) 109916
DOI:10.1016/j.jcsr.2025.109916
Status : Postprint (Author's version)

is the yielding strength of the end-palte.

Regarding the technological details, all critical welds (i.e., continuity plate to the column flange and beam flange to the end-plate) are full penetration welds, while fillet welds are used for other details (i.e., beam web to the end-plate and continuity plate to the column web) as shown in Fig. 2.

Fig. 2. *Types of adopted welds: (a) welds between the end-plate and the beam; (b) welds between the continuity plates and the column.*

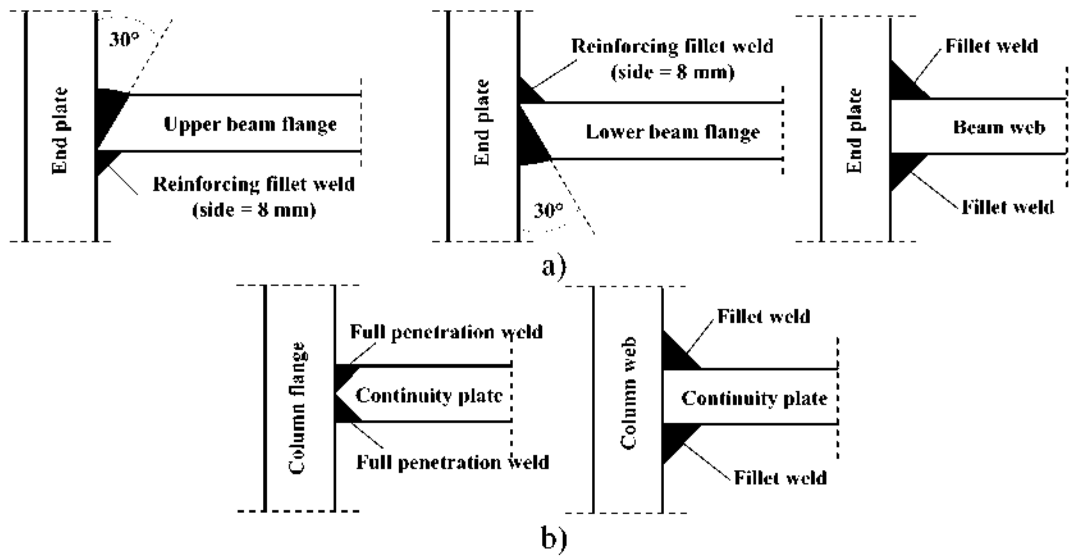

Table 1. *Design assumptions of the tested joints.*

Set of joints	Design criteria		Connection			Column web panel		Joint		
	Expected performance	Mb,pl,k	Mcon	Mcon/Mb,pl,k	Mcon/Mcwp	Mcwp	Mcwp/Mb,pl,k	Mj	Sj,ini	Mj/Mb,pl,k
		(kNm)	(kNm)	(-)	(-)	(kNm)	(-)	(kNm)	(kNm)	(-)
E1-TB-E	Balanced CWP/ Equal strength connection	361,6	446	1,23	1,21	368	1,02	368	71,577	1,02
E1-TB-P	Balanced CWP / Partial strength connection	361,6	394	1,09	1,07	369	1,02	369	69,051	1,02
E2-TB-E	Balanced CWP / Equal strength connection	604	743	1,23	1,22	611	1,01	611	127,267	1,01
E2-TB-P	Balanced CWP / Partial strength connection	604	579	0,96	0,95	612	1,01	579	114,885	0,96
E3-TW-E	Weak CWP / Equal strength connection.	1266,4	1197	0,95	1,04	1148	0,91	1148	248,861	0,91
E3-TW-P	Weak CWP / Partial strength connection	1266,4	945	0,75	0,83	1139	0,90	945	238,601	0,75

E1 assembly: Beam IPE360 – Column HEB280.
E2 assembly: Beam IPE450 – Column HEB340.
E3 assembly: Beam IPE600 – Column HEB500.

Published in : Journal of Constructional Steel Research 235 (2025) 109916
DOI:10.1016/j.jcsr.2025.109916
Status : Postprint (Author's version)

Table 2. *Geometrical and mechanical features of the tested joints.*

Specimen ID	Loading Protocol	End-Plate			Bolts (rows, diameter, and spacing)						Continuity Plates
		hEP (mm)	bEP (mm)	tEP (mm)	Bolt rows	d (mm)	e (mm)	w (mm)	p1 (mm)	p2 (mm)	tCP (mm)
E1-TB-E-C1	AISC341	590	280	20		27	65	140	122	–	18
E1-TB-E-C2	AISC341	590	280	20		27	65	140	122	–	18
E1-TB-E-M	Monotonic	590	280	20	4	27	65	140	122	–	18
E1-TB-P-C1	AISC341	590	280	15		27	65	140	122	–	18
E1-TB-P-C2	AISC341	590	280	15		27	65	140	122	–	18
E1-TB-Psp-C	AISC341	590	280	15	4	27	65	140	122	–	18
E2-TB-E-C1	AISC341	700	300	25		30	70	150	134	–	18
E2-TB-E-C2	AISC341	700	300	25		30	70	150	134	–	18
E2-TB-E-M	Monotonic	700	300	25	4	30	70	150	134	–	18
E2-TB-P-C1	AISC341	700	300	20		30	70	160	148	–	18
E2-TB-P-C2	AISC341	700	300	20		30	70	160	148	–	18
E2-TB-Psp-C	AISC341	700	300	20	4	30	70	160	148	–	18
E3-TW-E-C1	AISC341	910	300	25		36	80	150	164	90	20
E3-TW-E-C2	AISC341	910	300	25		36	80	150	164	90	20
E3-TW-E-Cej	EJ	910	300	25	6	36	80	150	164	90	20
E3-TW-P-C1	AISC341	910	300	20		36	80	150	164	90	20
E3-TW-P-C2	AISC341	910	300	20		36	80	150	164	90	20
E3-TW-Psp-C	AISC341	910	300	20	6	36	80	150	164	90	20

3. Experimental tests

3.1 Experimental program

Four sets of joints are investigated, and each set comprises three specimens with the same geometry, thus resulting in a total number of 18 specimens. The design criteria of each set of UEP joints are reported in Table 1, where the expected performance and the design resistances (see Section 2) of the connection and CWP are compared against the nominal plastic moment of the connected beams.

As it can be noted in the column "Design Criteria - Expected performance" of Table 1, the sets of joints E1/E2-TB-E are designed in order to promote yielding in both the column web panel and the end-plate connection, but with a greater contribution of CWP to the total joint

rotation. The sets of joints E1/E2-TB-P are designed in order to have greater plastic deformations in the end-plate connection than those potentially experienced by the joints of the former set. The E3-TW-E joints are designed to concentrate most of the plastic deformation in the CWP (which is designed as the weaker component). The E3-TW-P joints are designed to have the larger plastic deformation in the CWP but less damage than the previous case because the end-plate connection is expected to contribute more than the previous case (being weaker) to the overall rotation.

The geometrical features of each tested specimen are summarised in Table 2, where the specimens are univocally identified through the following labelling code:

E (Extended unstiffened) 1/2/3 (for joints with shallow/intermedi- ate/deep members, respectively) – TS (T-Shape, namely external joints) – E/P/Psp (Equal strength / Partial strength / Partial strength with shot peening of the welds) - C1/C2/C/CA/M (loading protocol, see Table 2).

All specimens were made of S355 steel grade, and high-strength preloaded 10.9 HV bolts with K2 class were used for all studied connections. In addition, three partial strength joints were manufactured using shot peening (see the specimens identified with the sub-code "Psp" in Table 2) for the end-plate-to-beam welds and the welds of continuity plates to column flanges to investigate the potential beneficial effect of such treatments on the ductility of partial strength connections that should develop plastic deformations. At least two cyclic tests have been performed per type of configuration by imposing the AISC341 protocol [27] (see in Table 1 the specimens with sub-ID "C1" and "C2" that refer to the first and the second test using the AISC341 protocol for two nominally identical specimens). Additionally, as indicated by the sub-ID "M" in Table 2, three monotonic tests have been performed in order to investigate the influence of the beam-to-column ratio on the monotonic resistance and rigidity of these joints. It is also worth noting that one cyclic test was carried out by applying an alternative loading protocol that was developed within the EQUALJOINTS project [16] (see in Table 1 the specimen with sub-ID "ej").

Published in : Journal of Constructional Steel Research 235 (2025) 109916
DOI:10.1016/j.jcsr.2025.109916
Status : Postprint (Author's version)

Fig. 3 gives the geometries of the tested joints, whose dimensions are also reported in Table 2 in terms of depth (h_{EP}), width (b_{EP}) and thickness (tEP). The bolt diameter (d), the vertical distance from the edge of the outermost bolt row (e), the horizontal distance between bolts (w), the spacing between the first and the second active bolt rows (p1), and the distance between the second and the third active bolt rows (p_2) are also reported for the bolted details (where the definition of active bolt rows is shown in Fig. 1). The thickness of the continuity plates (tCP) is also given, and no supplementary column web plates were used.

Fig. 3. *Geometrical features of investigated configurations.*

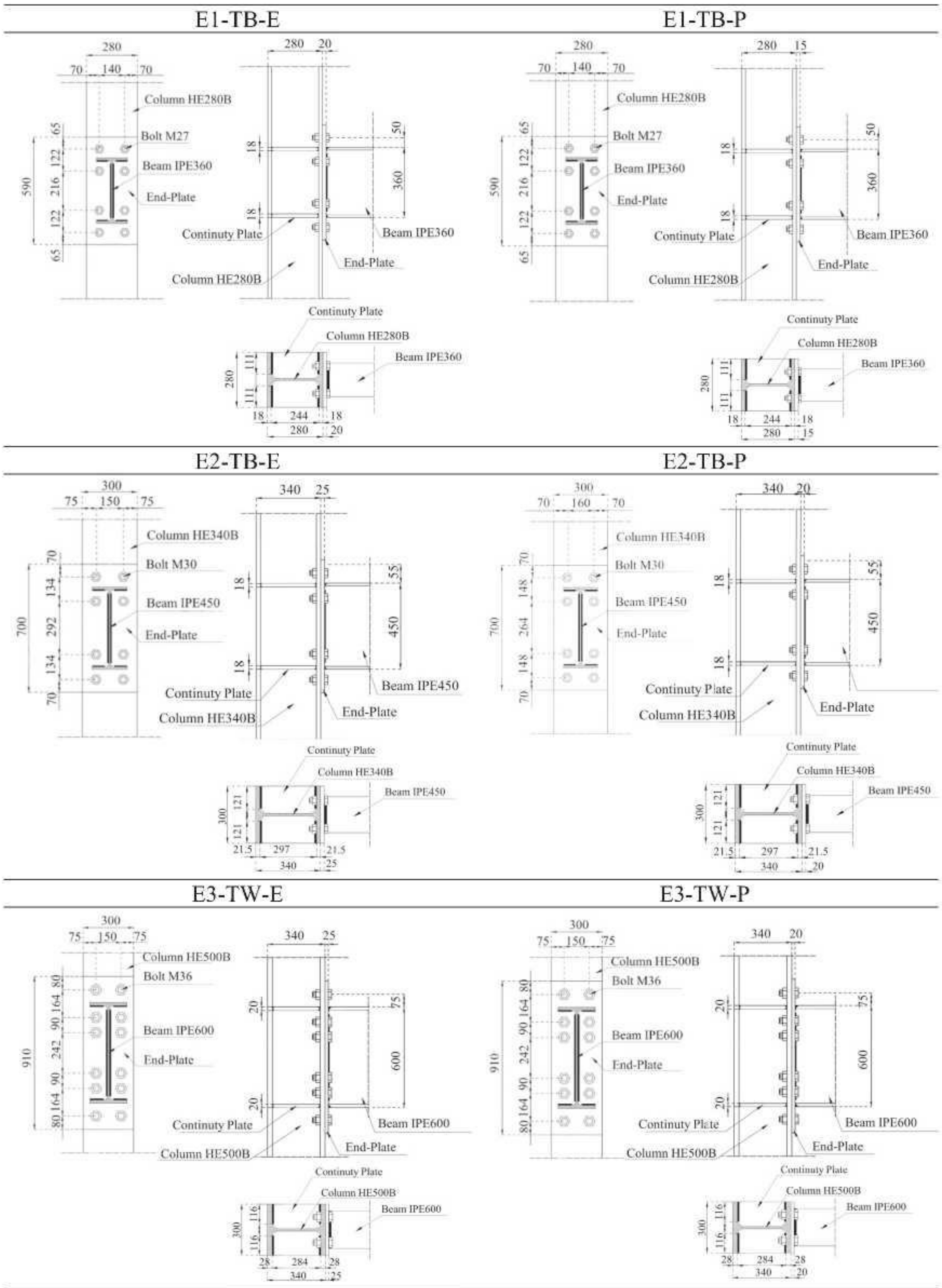

Published in : Journal of Constructional Steel Research 235 (2025) 109916
DOI:10.1016/j.jcsr.2025.109916
Status : Postprint (Author's version)

Fig. 4. *Experimental setup at UNINA (a and b) and ULiege (c and d).*

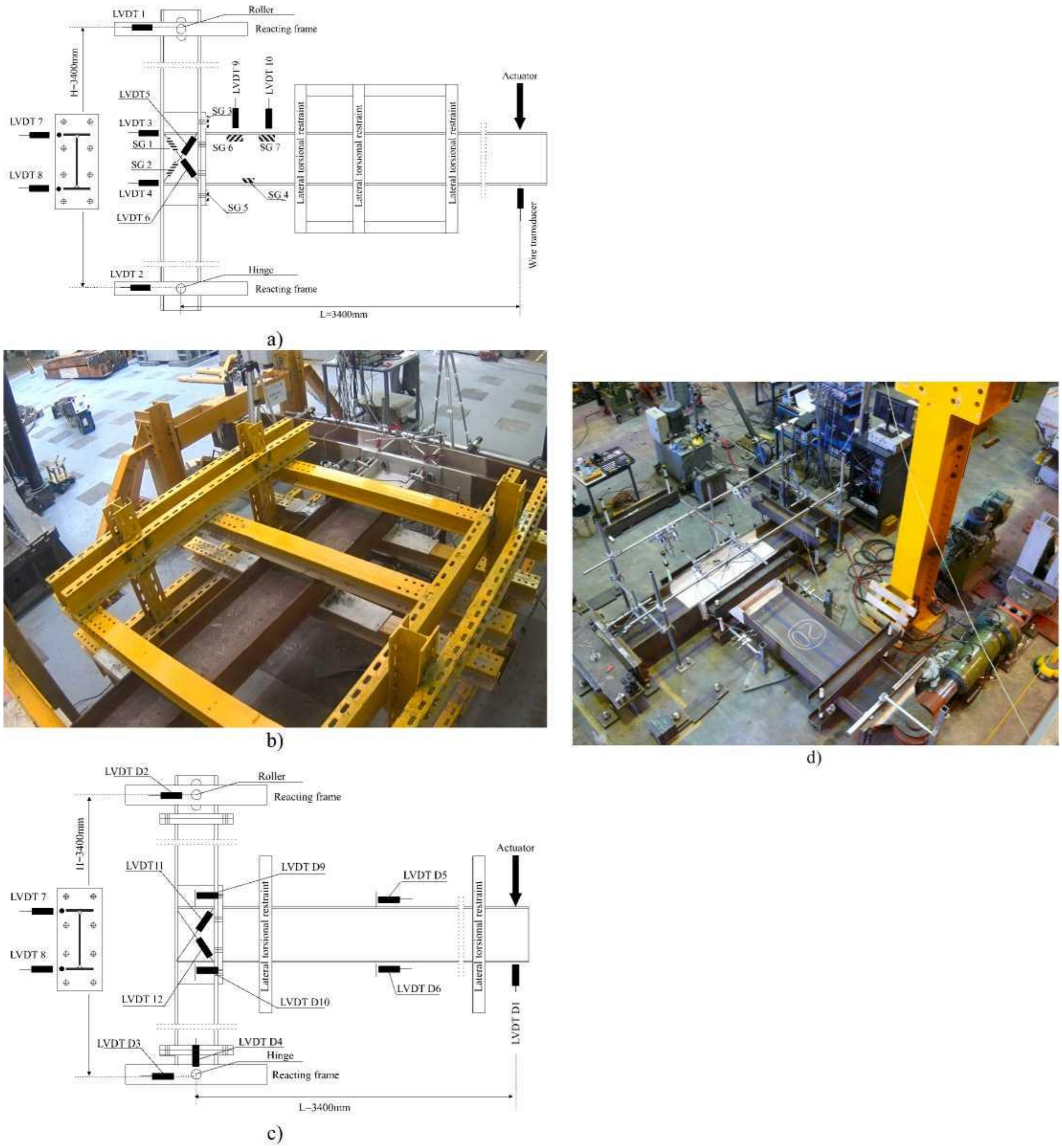

Published in : Journal of Constructional Steel Research 235 (2025) 109916
DOI:10.1016/j.jcsr.2025.109916
Status : Postprint (Author's version)

Fig. 5. *Adopted loading protocols for cyclic tests: AISC341 (a), alternative protocol (b) and comparison of cumulative demand functions (c).*

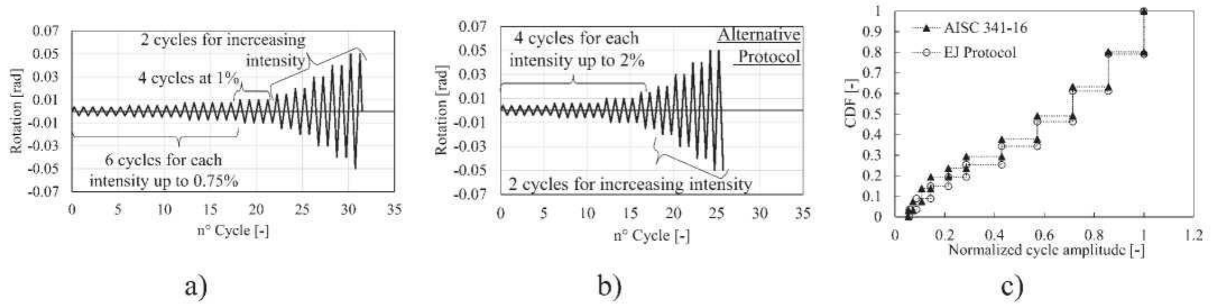

Fig. 6*. Acceptance criteria to qualify the tested joints.*

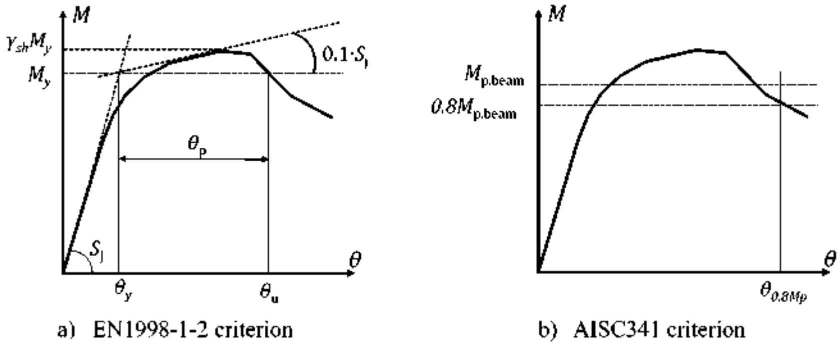

3.2 Experimental setup and testing procedure

The experimental setup and testing procedure are similar to those presented by the Authors in a previous experimental study [28]. For the sake of clarity, the main details are also given hereinafter. The six specimens of the E1 configurations were tested at the University of Naples Federico II (hereinafter also referred to as "UNINA"), and the adopted experimental setup is shown in Figs. 4a,b. The twelve specimens corresponding to E2 and E3 configurations were tested at the University of Liege (hereinafter also referred to as "ULiege") through the setup depicted in Fig. 4c,d. In both cases, the specimens were horizontally placed and restrained against lateral-torsional buckling by means of a reacting steel frame. The displacement history was applied through an actuator at the free tip of the beam, while the ends of the column were restrained by a pinned and a slider restraint, respectively, in order to mimic the boundary conditions of the sub-structured beam-column subassembly. Fig. 4 also shows the location of the displacement transducers that were used to measure the deformations of the specimens. During the tests, the interstorey drift angle θ = δ/L (being δ the displacement at the beam tip and L the length from the column axis to the beam tip) and bending moment M at the column axis were monitored; these data are available in the Annex of this article.

Strain gauges were also used to measure local deformations (see Fig. 4a), and linear variable displacement transducers were applied to measure the rotations of the column panel zone and the end-plate connection.

Regarding the imposed displacement histories, both monotonic and cyclic loading protocols were used. The AISC341 loading protocol was used to qualify the seismic performance of the joints (see Fig. 5a). In addition, the loading protocol developed in the RFCS EQUALJOINTS project [16] (hereinafter also referred to as "EJ" protocol) was also used for the sake of comparison. Fig. 5b shows the history of interstorey drift angle imposed by AISC341 [27] and EJ [16] protocols. Moreover, in order to highlight the difference between these two loading protocols, the normalised cumulative demand functions (CDF) defined in Eq. (6) as the number of cycles at imposed interstorey drift angle normalised to 0.04 rad were depicted in Fig. 5c. As it can be observed, despite the reduction in the number of cycles, the EJ protocol gives values of CDF similar to those of the AISC341 one.

$CDF = CDF_i/CDF_{0.04} = (CDF_{i-1} + n_{cycle} \bullet rot_i)\ /CDF_{0.04}$ (6)

Two acceptance criteria were also considered to discuss the seismic performance of the tested joints, namely according to prEN1998-1- 2:2022 [15] (see Fig. 6a) and AISC341 [27] (see Fig. 6b). In the first case, the joint shall provide at least a plastic rotation "θ_p" (see in Fig. 6a, to be evaluated without the elastic contribution "θy" of beam and column) greater than 0.03 rad for highly ductile structures (i.e., DC3 concept in prEN1998-1-2 [15]) or 0.02 rad for moderate ductile structures (i.e., DC2 concept in prEN1998-1-2:2022 [15]).

In the case of AISC341 [26], the joint shall withstand a moment not smaller than 80 % of the plastic flexural resistance of the beam at a story drift angle "θ0.8Mp" equal to 0.04 rad for highly ductile structures (i.e., special moment frames in AISC341 [27]) or 0.02 rad for moderate ductile structures (i.e., intermediate moment frames in AISC341 [27]). The joint can be qualified if it is able to experience at least one full cycle with the minimum requested rotation/storey drift.

3.3 Material properties

All steel parts of the specimens were built using S355 steel grade. Preloaded HR 10.9 bolts were used for the connections. The mean values of the actual mechanical properties of the materials are summarised in Table 3.

Table 3. *Mean values of the actual mechanical properties of the tested materials.*

Elements (profiles/plates / bolts)	Sampled location/ type	Elastic modulus (N/mm^2)	fy/fy,nom (-)	Yield stress (fy) (N/mm^2)	Ultimate stress (fu) (N/mm^2)	Elongation (%)
	Web	207,135	1.30	461.9	506.2	33.0
IPE 600	Flange	184,153	1.34	475.8	552.2	35.5
	Web	204,118	1.20	425.6	516.2	30.7
IPE 450	Flange	206,095	1.16	410.9	517.1	32.9
	Web	205,626	1.11	395.7	511.0	32.1
IPE 360	Flange	195,124	1.07	381.2	518.2	30.3
	Web	208,199	1.08	383.6	497.5	27.0
HEB 280	Flange	203,616	1.09	387.0	502.8	31.1
	Web	207,850	1.18	420.2	497.7	32.0
HEB 340	Flange	217,136	1.37	486.2	565.8	29.5
	Web	212,481	1.23	436.2	501.0	34.6
HEB 500	Flange	222,699	1.23	435.1	552.4	34.7
	tep = 15 mm	203,220	1.29	459.2	567.3	33.8
	tep = 18 mm	211,573	1.18	417.9	551.7	33.4
	tep = 20 mm	209,002	1.43	509.3	563.4	20.6
	tep = 25 mm	196,203	1.30	459.8	589.8	32.9
Plates	tep = 30 mm	211,254	0.97	344.5	485.6	41.3
	d = 27 mm	211,700	1.05	944.2	1172.7	2.6
Bolts	d = 30 mm	204,100	1.12	1009.4	1254.1	2.1

Published in : Journal of Constructional Steel Research 235 (2025) 109916
DOI:10.1016/j.jcsr.2025.109916
Status : Postprint (Author's version)

Fig. 7. *Experimental moment-interstorey drift angle response curves.*

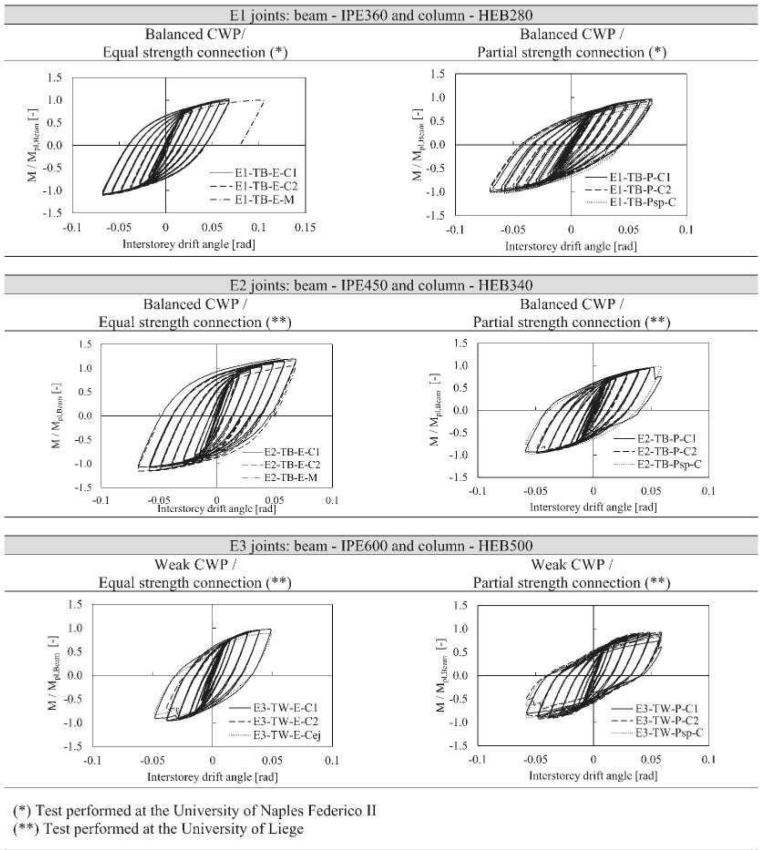

Fig. 8. *Failure modes of E1 joints at the first cycle imposed by the maximum stroke of the actuator.*

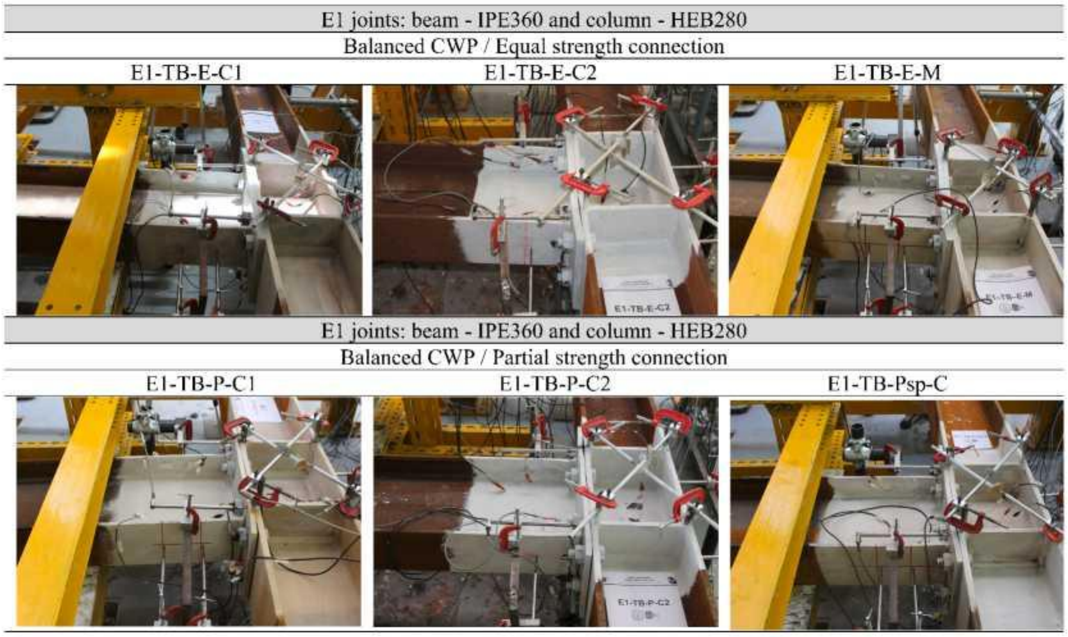

Published in : Journal of Constructional Steel Research 235 (2025) 109916
DOI:10.1016/j.jcsr.2025.109916
Status : Postprint (Author's version)

Fig. 9*. Pattern of cracks in the damaged joints at the end of the tests (i.e., for E1, E2 and E3 after the constant amplitude cycles at the maximum stroke of the actuator).*

Published in : Journal of Constructional Steel Research 235 (2025) 109916
DOI:10.1016/j.jcsr.2025.109916
Status : Postprint (Author's version)

Fig. 10. *Moment vs. interstorey drift angle, column web panel and connection rotation of the joints with equal strength connections.*

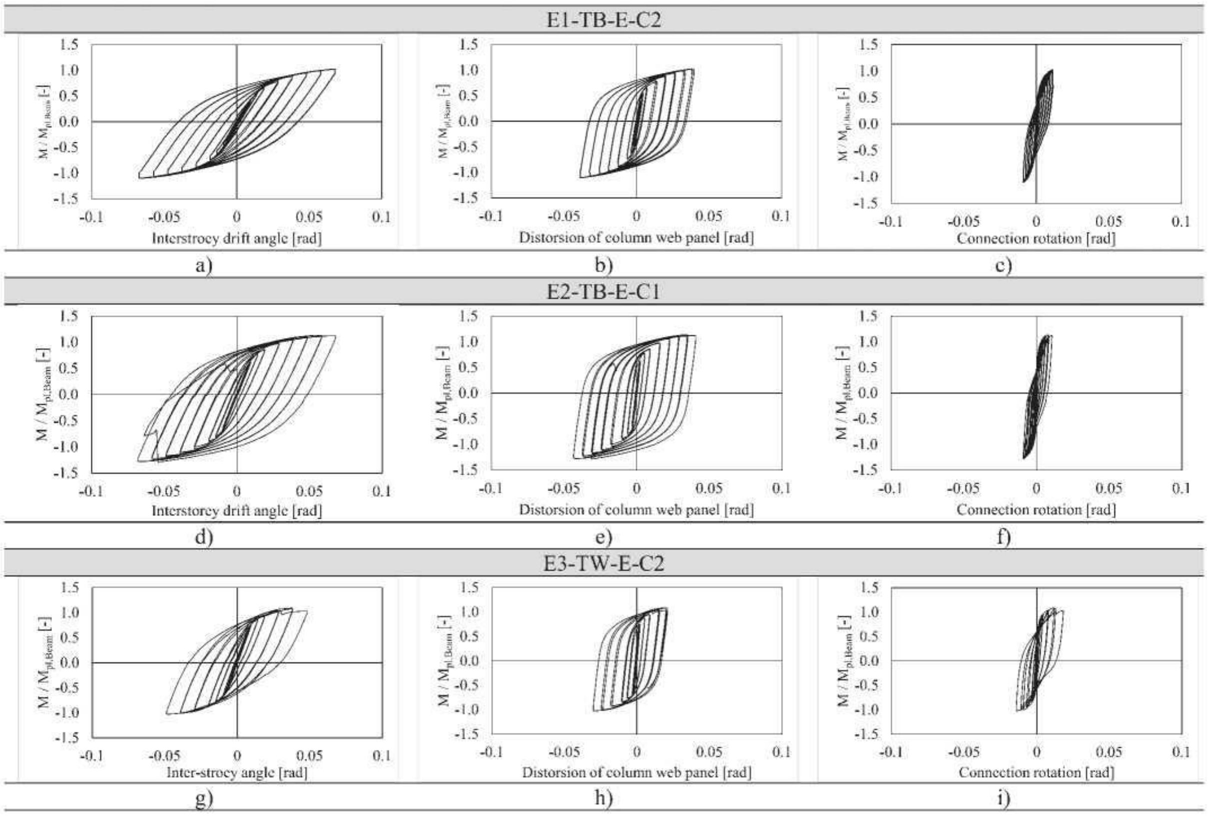

4. Experimental results

The experimentally measured moment at the column centreline vs. interstorey drift angle response curves are shown in Fig. 7. It is interesting to note that the hysteretic curves are rounded and stable without any degradation of the moment resistance up to 0.04 rad. Some pinching effects can be observed for E2 and E3 joints with partial strength connections because of the greater opening between the yielded end-plate and column flange.

No sign of degradation can be observed for all E1 joints up to about 0.07 rad under the AISC341 protocol (both those designed for balanced CWP and equal strength connection as well as those for balanced CWP and partial strength connection) and more than 0.10 rad under monotonic loading (the one designed for balanced CWP and equal strength connection). These joints with shallow beams are mainly characterised by the yielding of the column web panel and moderate opening of the end-plate (see Fig. 8). However, the beam flange-to-end-plate welds experienced severe cracking in the underbed zone and HAZ (Heat Affected Zone) toe that led to the full extraction of the welded core.

E2 and E3 joints exhibited the same types of plastic mechanisms and the ultimate damage pattern of the welds (see Fig. 9) but the failure of the beam flange-to-end-plate welds prematurely occurred at rotation of about 0.05 rad even though their cracking initiated at about 0.03 rad. These findings are mostly due to the large plastic deformation of the CWP as also observed by [29,30,31]. However, all tested joints exceeded the minimum performance limits requested by both EN1998-1-2 and AISC341 for DC3 and special frames, respectively.

The comparison between the hysteretic responses of E3-TW-E specimens (see Fig. 7) shows that the differences between tests using the AISC 341 [27] and the alternative EJ protocol [14] are negligible, as also observed for the tests carried out by the Authors on extended stiffened joints and reported in [28]. This finding is mainly due to the lesser elastic cycles of the EJ protocol with respect to AISC341.

Regarding the influence of shot peening, the experimental performance of the joints detailed with (i.e. those identified with the subscript "sp") and without such a treatment for the welds of the connection is substantially the same, thus confirming its ineffectiveness as formerly observed for extended stiffened connections in [28].

Published in : Journal of Constructional Steel Research 235 (2025) 109916
DOI:10.1016/j.jcsr.2025.109916
Status : Postprint (Author's version)

Figs. 10 and 11 show the hysteretic response curves of the CWP and connection of the tested joints (one per type for the sake of brevity, being almost the same per type of specimen).
As it can be observed, the joints with equal strength connection and balanced CWP (see E1-TB-*E*-C2 and E2-TB-E-C1 in Fig. 10) are characterised by small plastic engagement of the connection, while the most of energy dissipation is provided by CWP. In the cases of partial strength connections with balanced CWP (see E1-TB-P-C2 and E2-TB-P-C2 in Fig. 11), the weaker connection led to its slightly greater contribution to the energy dissipation (as testified by a bit larger size of the hysteretic loops and the values of their rotations). However, once again a larger amount of dissipation is provided by CWP.

The cases with designed weak CWP (i.e., E3-TW-*E*-C2 and E3-TW-P- C2) gave similar responses with a greater contribution of the connections with respect to the previous cases even though the design expected performance would have been different (namely lower plastic shear demand than the cases with designed balanced CWP). The reason for this unexpected behaviour is mainly ascribable to the inconsistency of the simplified assumptions of the design analytical model that considers an equivalent lever arm to compute MCWP and disregards the variation of shear forces of the inner bolt rows on the height of the column web panel. The importance of this effect to properly estimate the resistance of the joint when mechanical models are used has been recently clarified by Jaspart et Al. [32] and Golea et Al. [33], which showed that the inaccuracy is rather evident in the case of connections with more than one active inner bolt row, as for E3 specimens. In this regard, these observations motivated the recent review of the latest draft of EN1998-1-2 (i. e., prEN1998-1-2:2024 [34]), where this condition has been clearly stated and the simplified assumptions are permitted solely in the case of a single inner active bolt row (i.e., one active row below the bam flange in tension) for all bolted joints covered by that code.

Fig. 11. *Moment vs. interstorey drift angle, column web panel and connection rotation of the joints with partial strength connections.*

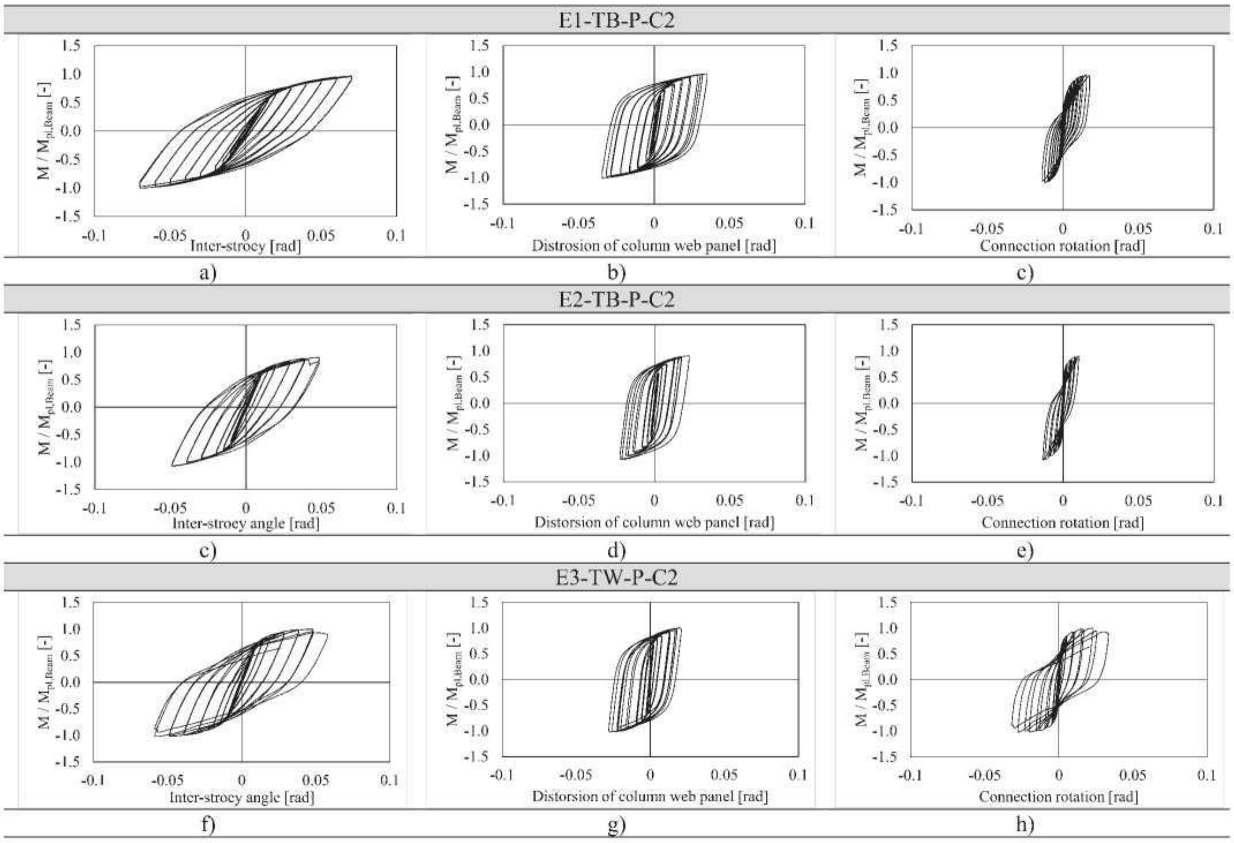

Published in : Journal of Constructional Steel Research 235 (2025) 109916
DOI:10.1016/j.jcsr.2025.109916
Status : Postprint (Author's version)

5. Seismic performance parameters vs pre-qualification limits

Fig. 12 shows the sagging (+) and hogging (-) backbone curves of the tested joints that are used to determine the response parameters depicted in Fig. 6, namely: the strain hardening factor (γ*h*), the yield interstorey drift angle (θ*y*), the ultimate interstorey drift angle (θ*u*), the plastic rotation (θ_p), the rotation ($\theta_{0.8Mp}$) and the dissipated cumulative
energy up to 0.04 rad ($DE_{0.04}$), which are all reported in Table 4. Moreover, as also reported by [35,36], the assemblies elastic stiffness was pointed out. In particular, in Table 4, the whole assembly elastic stiffness (SA) evaluated from the backbone curves, the experimental joint stiffness (S_J) (i.e., evaluated accounting for the contribution of the column web panel and the connection) and the analytical prediction, evaluated according to the component method (SJ,CM) were reported. As it can be observed, the CM provide an almost good prediction of the experimental joints' stiffness, especially for the E1 and E3 assemblies, while larger difference can be observed for the E2 specimens.

Since the tested joints do not exhibit appreciable strength degradation, the values of $\theta_{0.8Mp}$ correspond to the maximum rotations imposed by the test. In this regard, although not experimentally verified, it is presumable that these joints may potentially provide greater ductility than the values listed in Table 4.

The measured values of "θp" and "θ0,8Mp" confirm that all specimens satisfy the prequalification limits of EN1998-1-2 [15,34] as well as the deformation capacity required by AISC341 [27] for highly ductile structures, being greater than 0.03 rad and 0.04 rad.

It can be also observed that the strain hardening factor from cyclic tests varies from 1.26 to 1.37, as also observed by [37] for AISC- compliant joints. In the case of joints with Equal strength connection and balanced CWP (i.e., E1-TB-E and E2-TB-E specimens), the mean γsh is about 1.31 (coefficient of variation equal to 3.3 %). In the case of partial strength connection and balanced CWP (i.e., E1-TB-P and E2-TB- P specimens), the mean γsh is about 1.29 (coefficient of variation equal to 1.8 %). In all other cases (i.e., E3 specimens), the mean γ_sh is about 1.29 (coefficient of variation equal to 0.6 %). The mean value for all tested specimens is about 1.31 (coefficient of variation equal to 3.2 %).

Therefore, considering a rounded mean value of γsh equal to 1.3 and the EC8 value of γ_{rm} for S355 (i.e., the steel grade of the tested specimens) equal to 1.25, the overall over-strength factor ($\gamma_{rm} \times \gamma_{sh}$) to verify the non-yielding parts and the column of UEP joints can approximately be estimated as 1.25 × 1.3 = 1.63.

Regarding DE0.04 it can be noted that E1/E2-TB-E joints dissipated more energy than the E1/E2-TB-P because the former specimens exhibited larger plastic deformations in the CWP, which mostly contributed to the energy dissipation. A similar trend can be observed for the E3 assemblies, where the E3-TW-E dissipated more energy than E3-TW-P because of a similar contribution of CWP.

Fig. 12. *Sagging (+) and hogging (-) backbone of the moment vs. inter storey drift angle curves of E1 and E3 joints.*

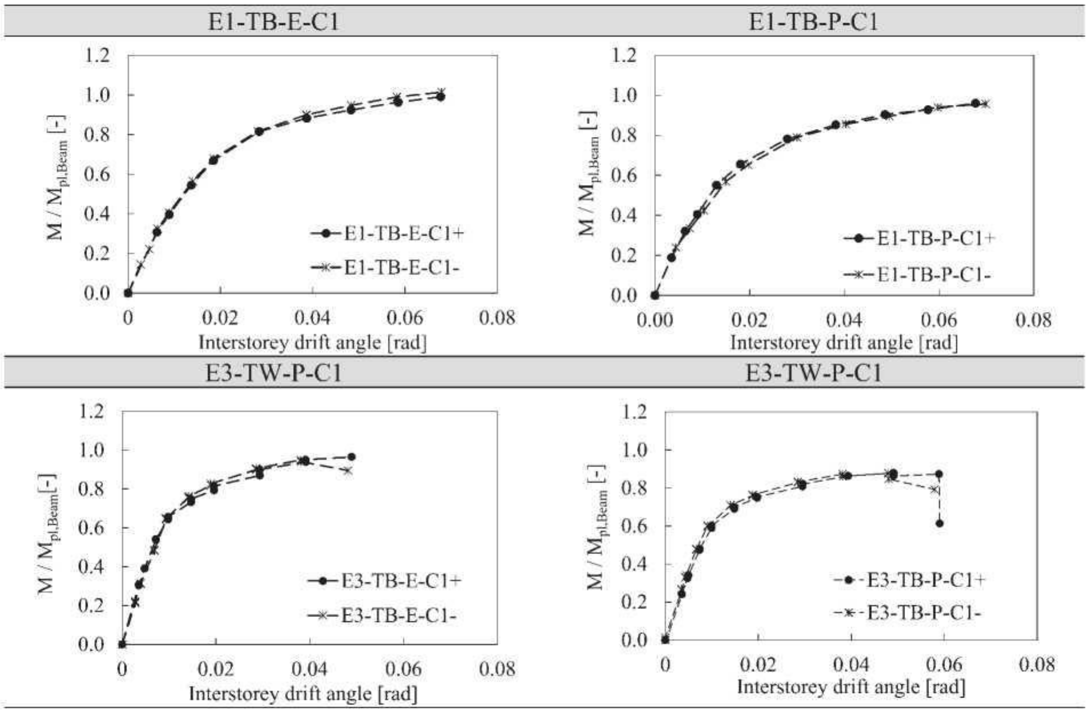

Published in : Journal of Constructional Steel Research 235 (2025) 109916
DOI:10.1016/j.jcsr.2025.109916
Status : Postprint (Author's version)

Table 4 *Performance parameters of the tested joints.*

Specimens	SA	Sj	Sj CM	γsh	θy	θu		θ0.8Mp	DE0.04
	[kNm]	[kNm]	[kNm]	[-]	[rad]	[rad]	[rad]	[rad]	[kJ]
E1-TB-E-C1	20,000	66,500		1.269	0.016	0.068*	0.052	0.068	61.4
E1-TB-E-C2	21,000	67,000	70,043	1.299	0.015	0.068*	0.053	0.068	59.5
E1-TB-E-M	20,000	68,500		1.410	0.015	0.105*	0.090	0.105	–
E1-TB-P-C1	20,000	60,500		1.297	0.015	0.068*	0.052	0.068	50.5
E1-TB-P-C2	19,000	60,000	67,435	1.292	0.016	0.070*	0.054	0.070	49.6
E1-TB-Psp-C	21,500	61,500		1.294	0.021	0.064**	0.043	0.064	48.5
E2-TB-*E*-C1	47,800	175,000		1.371	0.013	0.068*	0.056	0.068	137.4
E2-TB-E-C2	49,500	185,000	125,729	1.320	0.012	0.059**	0.046	0.059	145.5
E2-TB-E-M	48,000	195,000		1.360	0.012	0.068*	0.056	0.068	–
E2-TB-P-C1	42,000	160,000		1.306	0.012	0.059*	0.046	0.059	128.5
E2-TB-P-C2	37,000	150,000	111,630	1.261	0.014	0.049**	0.035	0.049	120.4
E2-TB-Psp-C	39,000	155,000		1.298	0.014	0.059**	0.045	0.059	118.2
E3-TW-*E*-C1	140,000	305,000		1.368	0.009	0.049**	0.040	0.049	337.8
E3-TW-E-C2	155,000	297,000	277,825	1.357	0.007	0.039**	0.032	0.039	322.7
E3-TW-E-Cej	135,000	295,000		1.310	0.009	0.049**	0.040	0.049	335.2
E3-TW-P-C1	107,800	285,000		1.283	0.010	0.059*	0.049	0.059	286.8
E3-TW-P-C2	107,800	287,000	268,546	1.309	0.011	0.059*	0.048	0.059	278.4
E3-TW-Psp-C	107,900	285,000		1.263	0.011	0.059*	0.048	0.059	295.7

(*) Maximum rotation permitted by the testing setup
(**) Prematurely interrupted due to technical problems with the testing setup.

6. FEM analyses

6.1 Modelling assumptions

Finite element Models (FEMs) were built using ABAQUS 6.17 [38], on the basis of the same assumptions formerly presented by the Authors in [28]. For the sake of clarity, the main hypotheses are described hereinafter.
The details of the modelled parts of a joint are depicted in Fig. 13. C3D8I solid elements (i.e., 8-node linear brick, incompatible mode) were used to discretise the geometries of the specimens through the structured-meshing technique. This type of element was preferred to the C3D8R elements because they are designed to handle bending and large deformations, providing more accurate predictions of stress and plasticity, despite the significant computational effort involved. The density of the mesh was selected by means of preliminary sensitivity analyses, as shown in Fig. 13b where the influence of mesh size on von Mises stress (VMS) at 6 % of interstorey drift angle is reported. Based on these results, the average size of the finite elements was assumed equal to 3.5 mm, 2.5 mm, and 10 mm for the end-plate, the bolts and the beam-end, respectively.

The contacts were modelled using surface-to-surface interactions with "Hard Contact" formulation for normal contact, and "Coulomb friction" for the tangential behaviour (the friction coefficient was set equal to 0.3). The experimental properties of the materials were used (see Table 3), and true stress-true strain curves were derived from the experimental engineering curves. Von Misses yielding criterion with combined hardening was adopted.

The out-of-square imperfections of the flanges of steel members were implemented by imposing the shape of the relevant buckling mode with an amplitude equal to 80 % of the maximum mill tolerances permitted by EN 10034 [39]. The material properties of the columns, beams and plates were imposed starting from the measured properties reported in Table 3.

The bolts were modelled as dumbbell shapes using non-linear behaviour and were simulated using the multilinear force-displacement curves given by [40] that were updated with measured material properties (see Table 3).

The pre-tensioning of bolts was modelled using the "Bolt load" option by imposing the actual value adopted to tighten the specimen (which was in accordance with EN1993–1-8). In particular, pre-tension loads equal to 321 kN 393 kN and 572 kN were adopted for 10.9 M27, M30 and M36 bolts, respectively.

All welds were modelled as solid elements with "Tie" constraints between the connected surfaces. In addition, their material was assumed as elastic perfectly plastic, with a yield stress equal to 460 MPa [41]. Moreover, the initiation of welds' fracture was monitored by means of a cyclic Void Growth Index as reported in Kanvinde et al. [42].

The boundary conditions and torsional restraints were consistent
with the sub-structuring shown in Fig. 4. Dynamic implicit analyses with quasi-static option were carried out in two steps, namely: 1) the bolt preload; 2) the displacement histories at the tip of the beam.

Published in : Journal of Constructional Steel Research 235 (2025) 109916
DOI:10.1016/j.jcsr.2025.109916
Status : Postprint (Author's version)

Fig. 13. *Details of the FE models: Adopted mesh (a) and mesh sensitivity (b to d).*

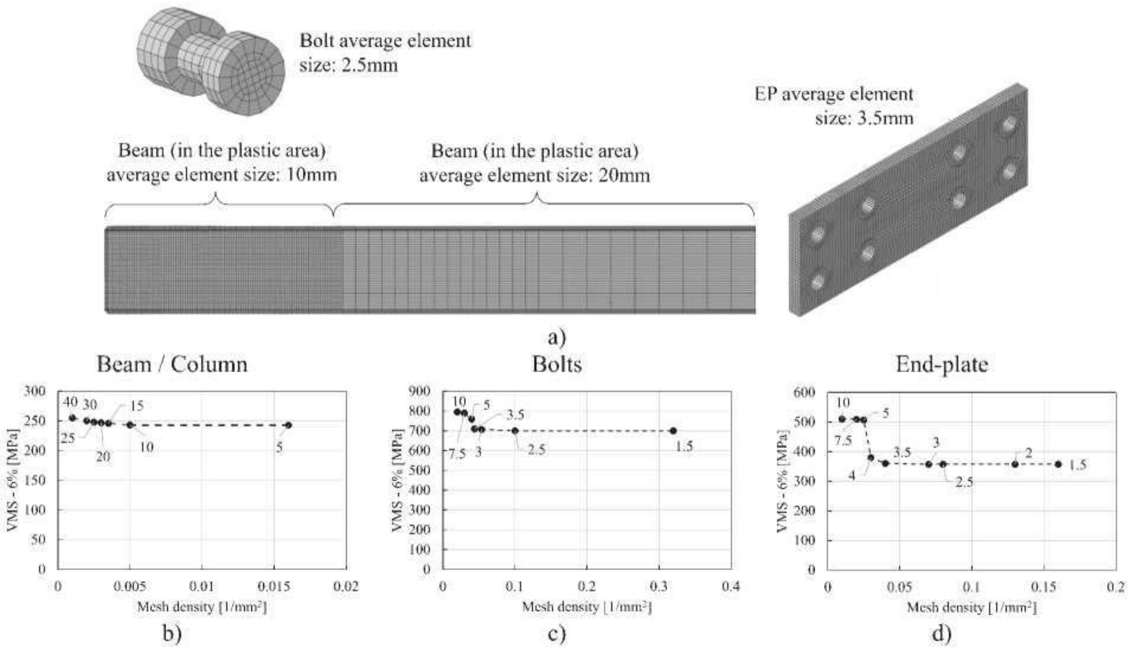

6.2 FE simulations vs. experimental results

The results of FE simulations are compared to those experimentally observed in terms of damage pattern and moment-rotation response curves. In addition, the local response of the numerical models is investigated through two damage indices: (i) PEEQ (equivalent plastic strain index); and (ii) RI (rupture index). The PEEQ is monitored to evaluate the amount of plastic deformation in the damaged zones and is computed by the following equation:

$$\mathrm{PEEQ} = \frac{\sqrt{\frac{2}{3}\varepsilon_{ij}^{p}\varepsilon_{ij}^{p}}}{\varepsilon_y} \qquad (7)$$

where ε_{ij}^{p} and εy are the tensor of plastic strains and uniaxial yield strain, respectively.

The RI is derived to assess the tendency to exhibit ductile rupture in the critical details. The RI index is derived as follows:

$$RI = \frac{PEEQ}{exp(-1.5T)} = \frac{PEEQ}{exp\left(-1.5\frac{\sigma_m}{\sigma_e}\right)} \qquad (8)$$

where σm and σe are the hydrostatic stress and Von Mises stress, respectively.

The comparison between the numerical and experimental responses of the examined specimens is depicted in Fig. 14. As it can be trivially recognised, all FE models satisfactorily mimic both the response curves and the damage pattern of the relevant tested joints.

The evolution of the PEEQ clearly confirms the activation of the expected plastic modes in E1 and E2 assemblies. In addition, the distributions of PEEQ in E3 specimens confirm the validity of the analytical models proposed by [32,33], because the CWPs of those joints are not uniformly yielded in shear but there is a major localization of plastic deformations into the central area of the CWP, namely between the inner bolt rows in the central part of the connection because of the variation of shear force at each bolt row.

Fig. 15 depicts the patterns of RI across the flange width (bf) at the beam flange to the end plate weld toe (for the sake of clarity, the RI indexes are given as a function of the normalised position x/bf where x is the location of the measured points of the beam width) for 2 %, 4 % and 6 % of interstorey drift angles. As observed, the RI indexes are smaller than 1 in all cases, thus confirming the ductility of these joints even though the RI are close to 1 at 6 % for E1 and E2 joints (i.e., those designed with equal strength or partial strength connection and balanced CWP). In those cases, when RI tends to 1, the models suggest the tendency to develop fractures in those welds, as also observed after the performed tests. In E3 assemblies, RI indexes largely decrease because of the lesser plastic deformation of the CWP, which results in a greater deformation of the end-plate and a lower demand to the beam end, with the beam depth, while full strength joints exhibit a different evolution of RI that is substantially greater in ES3 specimens. This observation is also in line with the experimental results.

Published in : Journal of Constructional Steel Research 235 (2025) 109916
DOI:10.1016/j.jcsr.2025.109916
Status : Postprint (Author's version)

Fig. 14. *FE simulations vs. experimental results.*

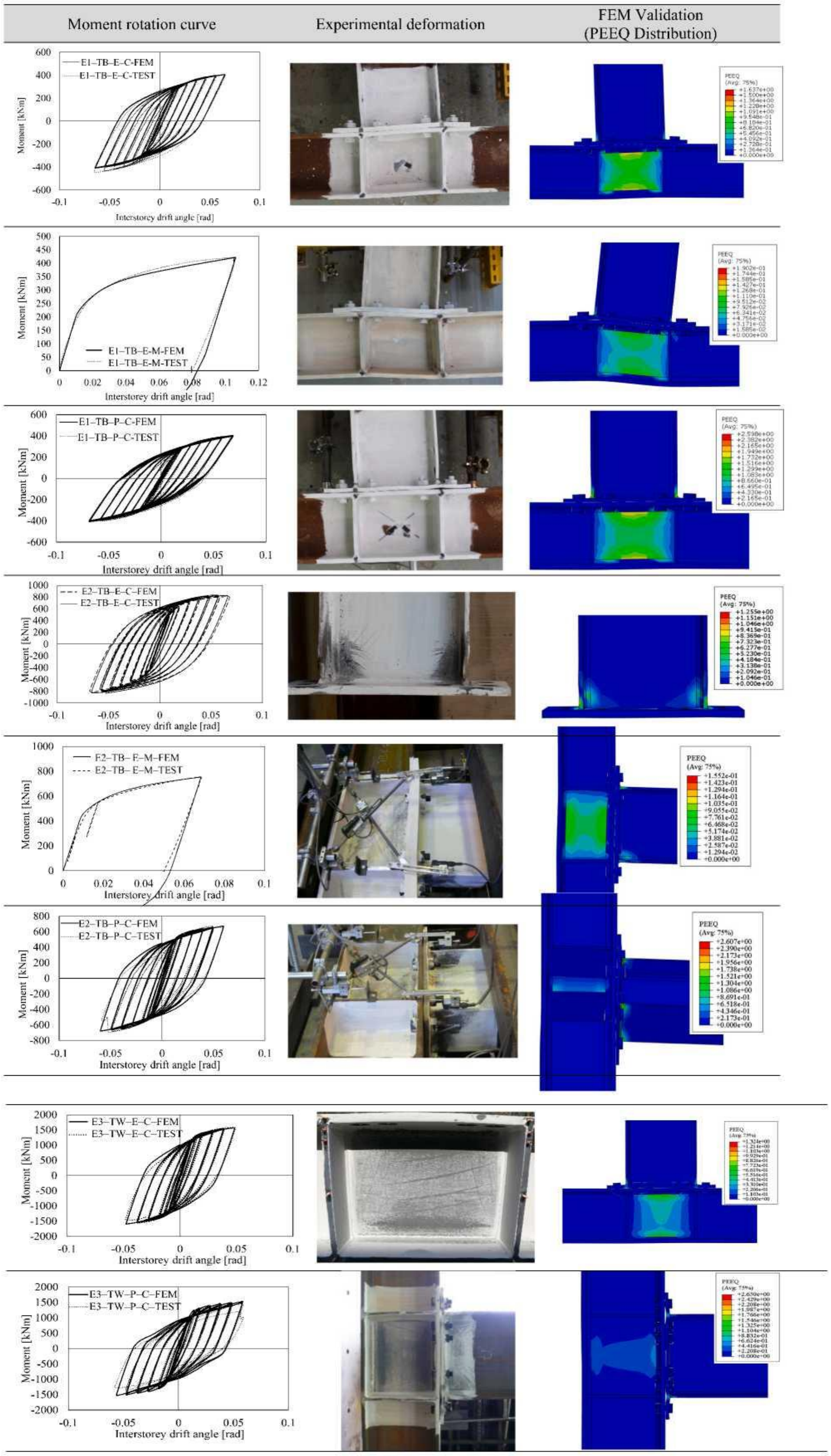

Published in : Journal of Constructional Steel Research 235 (2025) 109916
DOI:10.1016/j.jcsr.2025.109916
Status : Postprint (Author's version)

Fig. 15. *Evolution of RI across the beam width.*

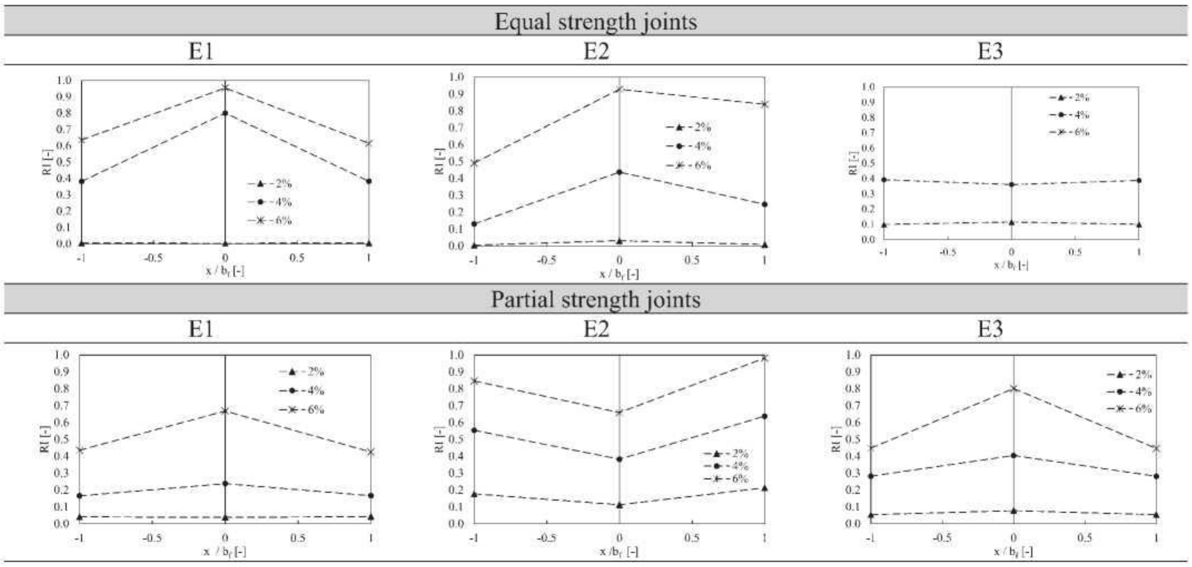

7. Conclusions

The present work aims to investigate the monotonic and cyclic performance of extended Unstiffened End-Plate (UEP) for their seismic prequalification in the framework of the latest versions of European codes (i.e., EN1998-1-2 and EN1993-1-8) by means of experimental and numerical analyses. Therefore, this study provides the background information about the rules for UEP joints given in Annex E of EN1998-1- 2.

Eighteen specimens were designed and subdivided into six homogeneous sets tested, comprising three nominally identical geometries. These sets of joints were designed (i) varying three beam-to-column assemblies; (ii) varying the number of bolt rows (i.e., four rows in
which only one outer and another inner the beam flange in tension; six rows with one outer and two inner the beam flange in tension); (iii) manufacturing three specimens by imposing shot-peening treatments to all welds; and (iv) varying the resistances of the column web panel (CWP) and connection. The joints were designed in accordance with the rules recently incorporated by the latest EN1998-1-2, and four design performances were considered: (a) balanced CWP and equal strength connection, (b) balanced CWP and partial strength connection, (c) weak CWP and equal strength connection, (d) weak CWP and partial strength connection.

Based on the presented outcomes, the following remarks are summarised:

- All tested joints exhibited ductile behaviour with a stable hysteretic response.
- The tests confirmed that plastic deformations mainly occurred in the column web panel and end-plate connection. The hysteretic performances are stable without strength degradation thanks to the absence of any local buckling phenomena.
- The observed experimental response was consistent with the expected design performance of all joints with four bolt rows.
- The local response of the joints with six-bolt rows differed from the expected design performance. The damage was not fully concentrated in the column web panel, but an appreciable contribution of the connections was observed. This unexpected behaviour is mainly due to the inconsistency of the simplified assumptions of the design analytical model that disregards the variation of shear forces on the height of the column web panel. However, the overall behaviour was still very ductile.
- The large plastic deformations of the column web panel in all tested joints provided large ductility but also contributed to the formation of cracks in the welds, even though at large interstorey drift angles (about 0.04 rad).
- The mean measured strain hardening factor γ_{sh} was about 1.31, thus suggesting to consider the value 1.3 in the application of the capacity design of the non-yielding members and components of these joints.
- The results of finite element analyses confirmed the experimental observations. In particular, the full shear plastification of the column web zone in the joints with four bolt rows, while the localisation of plasticity in the central portion of the panel zone (i.e., between the two internal rows at the horseback of the centroid of the connection) in the case of joints with six-bolt rows. This result confirms that disregarding the variation of the shear forces in the column panel zone can lead to inaccurate

analytical predictions.

- The concentration of plastic deformations in the end-plate-to-beam weld was also confirmed by the finite element simulations. However, the rupture indexes do not exceed the value equal to one at 0.06 rad, thus confirming the experimental evidence. Further studies are deemed useful to further improve the ductility of such a detail.
- All joints provided a large ductility fully compatible with the required performance of both moment frames and dual frames. Therefore, in dual frames or in moment frames in low seismic areas, the use of such a type of joints can be effectively implemented in order to guarantee both redundancy and ductility as well as to have cheaper constructional details in comparison to a full strength connection.

CRediT authorship contribution statement

Roberto Tartaglia: Writing - review & editing, Visualization, Validation, Software, Investigation, Formal analysis, Data curation, Conceptualization, Methodology, Writing – original draft. **Mario D'Aniello:** Writing - review & editing, Writing - original draft, Visualization, Validation, Supervision, Project administration, Methodology, Investigation, Formal analysis, Data curation, Conceptualization. **Jean- François Demonceau:** Writing - review & editing, Visualization, Validation, Supervision, Methodology, Investigation, Formal analysis, Data curation. **Raffaele Landolfo:** Writing - review & editing, Visualization, Validation, Supervision, Resources, Project administration, Funding acquisition.

Declaration of competing interest

None.

Acknowledgments

The research activity presented in this paper received funding from the European Union's Research Fund for Coal and Steel (RFCS) research program under the following grant agreements:

- n° RFSR-CT-2013-00021- European pre-QUALified steel JOINTS: EQUALJOINTS;
- n° 754048 — EQUALJOINTS-PLUS — RFCS-2016.

Appendix A. Supplementary data

Supplementary data to this article can be found online at https://doi. org/10.1016/j.jcsr.2025.109916.

Data availability

Data will be made available on request.

References

[1] D. Beg, E. Zupancic, I. Vayas, On the rotation capacity of moment connections, J. Constr. Steel Res. 60 (3–5) (2004) 601–620.
[2] P. Zoetemeijer, Design method for the tension side of statically loaded, bolted beam-to-column connections, Heron 20 (1) (1974).
[3] J. Swanson, R. Leon, Bolted steel connections: tests on T-stub components, J. Struct. Eng. 126 (1) (2000) 91–99.
[4] V. Piluso, C. Faella, G. Rizzano, Ultimate behavior of bolted T-stubs. I: theoretical model, J. Struct. Eng. 127 (6) (2001) 686–693.
[5] V. Piluso, C. Faella, G. Rizzano, Ultimate behavior of bolted T-stubs. II: model validation, J. Struct. Eng. 127 (6) (2001) 694–704.
[6] J.A. Swanson, Ultimate strength prying models for bolted T-stub connections, Eng. J. 39 (3) (2002) 136–147.
[7] A.B. Francavilla, M. Latour, V. Piluso, G. Rizzano, Bolted T-stubs: a refined model for flange and bolt fracture modes, Steel Compos. Struct. 20 (2) (2016) 267–293.
[8] D. Kukla, A. Kozlowski, B. Miller, D. Ziaja, D. Nykiel, Experimental investigation of steel beam-to-column end-plate joints under static and impact loading, J. Constr. Steel Res. 212 (2024) 108241.
[9] A.B. Francavilla, M. Latour, P.J. Tan, G. Rizzano, Ultimate behaviour of bolted beam-to-column connections in large rotations, J. Constr. Steel Res. 208 (2023) 108006.
[10] M. Morrison, D.Q. Schweizer, S. Quayyum, T. Hassan, Unstiffened eight-bolt extended end-plate moment connection for special and intermediate moment frames, J. Struct. Eng. 144 (2) (2018), https://doi.org/10.1061/(ASCE)ST.1943-

541X.0002332.
[11] M. Morrison, D. Schweizer, S. Quayyum, T. Hassan, Seismic analysis of eight bolt unstiffened end plate moment connection for special and intermediate moment frames, J. Struct. Eng. 145 (3) (2019) 04018123, https://doi.org/10.1061/(ASCE) ST.1943 541X.0003293.
[12] EN 1993-1-8, Design of steel structures - Part 1–8: Design of joints, 2005.
[13] CEN/TC 250/SC 3 N 3840, FprEN 1993-1-8:2022 - Eurocode 3: design of steel structures — part 1-8: joints, 2025.
[14] EN 1990, Eurocode: Basis of structural and geotechnical design, 2025.
[15] prEN1998-1-2, Eurocode 8: Earthquake resistance design of structures, CEN/TC 250/SC 8:2022, 2025.
[16] R. Landolfo, European seismic prequalification of steel beam-to-column joints: EQUALJOINTS and EQUALJOINTS-Plus projects, J. Constr. Steel Res. 192 (2022) 107238.
[17] R. Tartaglia, M. D'Aniello, G.A. Rassati, Proposal of AISC-compliant seismic design criteria for ductile partially-restrained end-plate bolted joints, J. Constr. Steel Res. 159 (2019) 364–383, https://doi.org/10.1016/j.jcsr.2019.05.006.
[18] R. Tartaglia, M. D'Aniello, G.A. Rassati, J.A. Swanson, R. Landolfo, Full strength extended stiffened end-plate joints: AISC vs recent European design criteria, Eng. Struct. 159 (2018) 155–171, https://doi.org/10.1016/j.engstruct.2017.12.053.
[19] American Institute of Steel Construction, Prequalified Connections for Special and Intermediate Steel Moment Frames for Seismic Applications (ANSI/AISC 358–22), AISC, Chicago, 2022.
[20] R. Tartaglia, M. Zimbru, M. D'Aniello, R. Landolfo, Finite element simulations on the ultimate response of extended stiffened end-plate joints, Steel Compos. Struct. 27 (6) (2018) 727–745, https://doi.org/10.12989/scs.2018.27.6.727.
[21] L. Mak, A. Elkady, Experimental database for steel flush end-plate connections, J. Struct. Eng. 147 (7) (2021) 04721006, https://doi.org/10.1061/(ASCE)ST.1943- 541X.0003064.
[22] D.A. Nethercot, Steel Beam to Column Connections - a Review of Test Data and their Applicability to the Evaluation of the Joint Behaviour of the Performance of Steel Frames, Report No. RR1084, University of Sheffield, Sheffield, UK, 1984.
[23] N. Kishi, W.-F. Chen, Data Base of Steel Beam-to-Column Connections, Structural Engineering Area, School of Civil Engineering, Purdue University, Indiana, USA, 1986. Report No. CE-STR-86-26.
[24] W.-F. Chen, N. Kishi, Semi rigid steel beam to column connections: database and modeling, J. Struct. Eng. 115 (1) (1989) 105–119.
[25] K.M. Abdalla, W.-F. Chen, Expanded database of semi-rigid steel connections, Comput. Struct. 56 (4) (1995) 553–564, https://doi.org/10.1016/0045-7949(94) 00558-K.
[26] K. Weynand, et al., SERICON – A databank for tests on semi-rigid joints, in: COST C1: Control of the Semi-Rigid Behavior of Civil Engineering Structural Connections, Office for Official Publications of the European Communities, 1999.
[27] AISC (American Institute of Steel Construction), Seismic Provisions for Structural Steel Buildings, ANSI/AISC 341-16, Chicago, IL, 2016.
[28] M. D'Aniello, R. Tartaglia, R. Landolfo, J.-P. Jaspart, J.-F. Demonceau, Seismic prequalification tests of EC8-compliant external extended stiffened end-plate beam-to- column joints, Eng. Struct. 291 (2023) 116386, https://doi.org/10.1016/J. ENGSTRUCT.2023.116386.
[29] R.M. Ghobarah, A. Korol, Osman, cyclic behavior of extended end-plate joints, J. Struct. Eng. 118 (1992) 1333–1335.
[30] A. Ghobarah, R.M. Osman, Korol, behaviour of extended end-plate connections under cyclic loading, Eng. Struct. 12 (1990) 15–27.
[31] P. Nogueiro, L. Simoes da Silva, R. Bento, R. Sim**o**es, Experimental behavior of standardized European end-plate beam-to-column steel joints under arbitrary cyclic loading, in: Proceeding of Stability and ductility of steel structures. Lisbon, Portugal, September 6–8, 2006.
[32] J.-P. Jaspart, A. Corman, J.-F. Demonceau, Characterization of unstiffened column webs in transverse compression in steel beam-to-column joints, Thin-Walled Struct. 180 (2022) 109848.
[33] T. Golea, A. Corman, J. Mathieu, Y. Duchene, J.-P. Jaspart, J.-F. Demonceau, An innovative mechanical model for structural steel joints, Eng. Struct. 277 (2023) 115459.
[34] CEN/TC 250/SC 8 N 1385, FprEN1998-1-2_draft_20-12-2024, Eurocode 8 — Design of structures for earthquake resistance — Part 1–2: Buildings, 2025.
[35] B.M. Abar, M.S. Ghobadi, New generation of bolted bracket connections: safe loadcarrying capacity and structural damage assessment, Eng. Struct. 252 (2022) 113662.
[36] M.S. Ghobadi, B.M. Abar, Development of new fully restrained bolted bracket moment connections for strong joints, Arch. Civil Mech. Eng. 21 (2021) 145.
[37] A. Yasin Onuralp Ozkılıç, Cem Topkaya, The plastic and the ultimate resistance of four-bolt extended end-plate connections, J. Constr. Steel Res. 181 (2021) 106614.
[38] Dassault Systemes, Abaqus Analysis 6.14 User's Manual, Simulia Inc., 2015.
[39] CEN 1993, CEN (European Committee for Standardization), Structural steel I and H sections: tolerances on shape and

dimensions, EN 10034, Brussels, 1993.

[40] M. D'Aniello, D. Cassiano, R. Landolfo, Simplified criteria for finite element modelling of European preloadable bolts, Steel Compos. Struct. Int. J. 24 (6) (2017) 643–658, https://doi.org/10.12989/scs.2017.24.6.643.

[41] ISO 14341:2020, Welding consumables. Wire electrodes and weld deposits for gas shielded metal arc welding of non alloy and fine grain steels, 2025.

[42] A.M. Kanvinde, G.G. Deierlein, Cyclic void growth model to assess ductile fracture initiation in structural steels due to ultra low cycle fatigue, J. Eng. Mech. 133 (6) (2007) 701–712.